Kinetic Study in a Microwave-Induced Plasma Afterglow of the Cu (^{2}S) Atom Reaction with CH_3Br at Temperatures between 300 and 804 K and with CH_3I between 300 and 696 K

Chris Vinckier* and Inge Vanhees

Department of Chemistry, KU Leuven, Celestijnenlaan 200F, B-3001 Leuven, Belgium

Received: October 17, 1997; In Final Form: December 16, 1997

A kinetic study of the reactions Cu + CH_3Br → CuBr + CH_3 (k_1) and Cu + CH_3I → CuI + CH_3 (k_2) has been carried out in a fast-flow reactor. The gas-phase copper atoms were generated using the microwave-induced plasma (MIP) afterglow technique. Atomic absorption spectroscopy at 327.4 nm was used as the detection technique. The influence of experimental parameters such as the hydrogen content, sublimation temperature of the CuCl pellet, and reactor pressure on k_1 and k_2 has been verified. The rate constant k_1 was measured at temperatures between 300 and 804 K, which resulted in the Arrhenius expression $k_1 = (1.7 \pm 0.2) \times 10^{-11} \exp[(-8.2 \pm 0.5 \text{ kJ mol}^{-1})/RT]$ cm^3 molecule^{-1} s^{-1}. Since the Arrhenius plot shows a slight curvature, the values of k_1 were also fitted to the modified Arrhenius equation $k(T) = A\,T^n \exp(-E/RT)$. Meaningful kinetic parameters can only be derived when n is fixed. The measured values of k_1 can be best described as a function of temperature over the 300−804 K range by the expression $\log k_1(T) = +223.6669 - 264.2058(\log T) + 97.7693(\log T)^2 - 11.9244(\log T)^3$. The Arrhenius expression for rate constant k_2 is $k_2 = (7.9 \pm 0.5) \times 10^{-11} \exp[(-0.8 \pm 0.2 \text{ kJ mol}^{-1})/RT]$ cm^3 molecule^{-1} s^{-1} between 300 and 696 K. The obtained results will be discussed in terms of the electron-jump model, and some reactivity/structure relations will be presented.

Introduction

The reactions of halomethanes with alkali-metal atoms have been investigated for more than 60 years. In the early 1930s Polanyi[1] and his collaborators studied reactions of alkali metals with several halogenated molecules in a diffusion flame. Numerous studies have been carried out using molecular beam techniques to determine the reaction cross sections. For the reactions with CH_3I the following cross sections were obtained:[2] 27 Å^2 (Li), 5 Å^2 (Na), and 35 Å^2 (K). The reactions of Na and K atoms with CH_3Br resulted in values of 6 and 3 Å^2, respectively.[3] To explain the reactivity of Na atoms with halomethanes, the electron-jump model was introduced.[4,5] According to this electron-jump or harpooning mechanism, a metal atom throws out its valence electron, which is then captured by the molecule. The distance r_c where the covalent potential-energy surface crosses the ionic potential-energy surface is given by[4]

$$\frac{e^2}{r_c} = \text{IE(Me)} - \text{EA(XY)} \qquad (1)$$

where e is the electronic charge, IE(Me) the ionization energy of the metal, and EA(XY) the electron affinity of the molecule XY, which represents a halogen molecule X_2 or an alkyl halide RX.

Halomethanes are well-suited for a systematic study such as testing the effect of electronegative substituents on reactivity.[6,7] The reaction of Cu atoms with CH_3Cl has already been studied at our laboratory.[8] In the present work the reactions of copper atoms with methyl bromide and methyl iodide have been investigated.

$$\text{Cu}\,(4^2\text{S}) + \text{CH}_3\text{Br}\,(^1\text{A}_1) \xrightarrow{k_1} \text{CuBr}\,(^1\Sigma^+) + \text{CH}_3\,(^2\text{A}''_2) \qquad (2)$$

$$\Delta H_r = -37.6 \text{ kJ mol}^{-1}$$

$$\text{Cu}\,(4^2\text{S}) + \text{CH}_3\text{I}\,(^1\text{A}_1) \xrightarrow{k_2} \text{CuI}\,(^1\Sigma^+) + \text{CH}_3\,(^2\text{A}''_2) \qquad (3)$$

$$\Delta H_r = +38.6 \text{ kJ mol}^{-1}$$

For both reactions 2 and 3 the kinetic study has been carried out in a fast-flow reactor. The microwave-induced plasma (MIP) afterglow technique was used as a source of the copper atoms in the gas phase.[9,10] Reaction 2 has been studied in the temperature range from 300 to 804 K, while reaction 3 has been followed between 300 and 696 K. An Arrhenius expression for k_1 and k_2 will be derived. There are no other kinetic data on these copper atom reactions available yet in the literature, but the results will be compared with similar potassium atom reactions. The Arrhenius parameters will be used as the basis for a number of reactivity/structure relationships.

Experimental Technique

Only the essential characteristics of the technique will be given here, since a detailed description of the experimental setup has been published previously.[11] The copper reactions were studied in a fast-flow reactor, which consists of a quartz tube with an internal diameter of 5.7 cm and a length of 100 cm. At the upstream end, a sample holder carries a CuCl pellet. A Kanthal resistance wire allows this solid pellet to heat up to a temperature T_s of about 800 K, independently of the temperature T_g in the reaction zone. The carrier gas argon transports the

S1089-5639(97)03386-0 CCC: $15.00
Published on Web 02/03/1998

evaporated copper chloride oligomers $Cu_xCl_{x,g}$ downstream, where they are mixed with the reaction products of a hydrogen/argon microwave-induced plasma (MIP) afterglow. Hydrogen atoms convert a fraction of the $Cu_xCl_{x,g}$ molecules into Cu atoms following a still unknown reaction sequence:

$$Cu_xCl_{x,g} + H \rightarrow ... \rightarrow ... \rightarrow Cu_g + \text{products} \qquad (4)$$

Atomic absorption spectroscopy at 324.7 nm was used to detect the copper atoms in the kinetic zone. Initial absorbances were kept below 0.3, which corresponds to a copper atom concentration of 4.3×10^{10} atoms cm^{-3} as an upper limit. However, the CH_3Br and CH_3I concentrations were orders of magnitude higher, which resulted in pseudo-first-order conditions for copper atom decays.

In the kinetic zone, the temperature T_g of the gas phase can be varied between 300 and 1000 K. The flow velocity v of the carrier gas argon was 324 ± 5 cm s^{-1} at 298 K. While the detection system remains at a fixed position, the fast-flow reactor assembly is mounted on a carriage which allows a horizontal displacement, so that copper absorbances can be measured along the reactor axis.

During the kinetic measurements several known amounts of the reagent (CH_3Br or CH_3I) were added through the additive inlet. For each amount the decay of the copper atoms was followed as a function of the axial distance (z) and thus of the reaction time (t) because $t = z/v$.

Gas flows were regulated by using Brook's precision needle valves of the ELF type or Brook's mass flow controllers, model 5850 E.

The gases used were argon (5.0) from UCAR with a purity better than 99.999%, mixtures of 1.02% and 5.3% CH_3Br in ultrahigh-purity argon (Praxair), and mixtures of 477.1 vpm and 0.538% CH_3I in UHP argon (BOC). Hydrogen was added as a 0.998% mixture in UHP argon (L'Oxhydrique), a 4.95% mixture in UHP helium (UCAR), or with a purity better than 99.9997% (L'Air Liquide).

Regression plots and statistical analyses were made by using the SAS-6.08 statistical package[12] available at our University Computer Centre. We have quoted the 1 σ standard error.

Results

Cu + CH_3Br Reaction. *Kinetic Expression for the Derivation of k_1.* The rate constant of reaction 2 can be determined from the copper atom decays as a function of the reaction time at various amounts of CH_3Br added. The formalism used for the derivation of k_1 is the same as in our previous work on the kinetics of copper,[8,10,11,13] sodium,[14] and magnesium[15,16] reactions:

$$\ln A_{Cu} = -\left\{\frac{k_1[CH_3Br]}{\eta} + \frac{7.34D_{Cu,Ar}}{2r^2}\right\}t + B \qquad (5)$$

in which A_{Cu} is the copper absorbance, k_1 the rate constant of reaction 2, η a correction factor (depending on the flow characteristics), $D_{Cu,Ar}$ the binary diffusion coefficient of copper atoms in the carrier gas argon, r the reactor radius, t the reaction time ($=z/v$), and B an integration constant. A complete discussion on the mathematics behind eq 5 is given by Howard et al.,[17] and the influence of the various flow characteristics on the magnitude of η is discussed by Fontijn et al.[18] This factor η takes into account the absence of plug flow conditons. In argon the flow has neither a plug flow ($\eta = 1$) nor a parabolic ($\eta = 1.6$) character. The extensive arguing for selecting the value of η will not be repeated here, but in our experimental conditions it is safe to set its value equal to 1.3 with an associated systematic error of 10%.

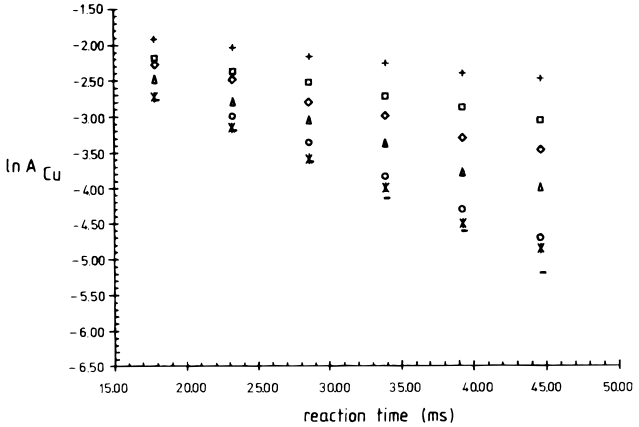

Figure 1. Natural logarithm of the Cu absorbance as a function of the reaction time. Experimental conditions: $T_g = 516$ K, $P_r = 9$ Torr, $T_s = 537$ K, $[H_2] = 9.9$ mTorr, and the carrier gas is argon. The CH_3Br concentrations are (+) 0, (□) 0.47, (◇) 1.11, (△) 1.75, (○) 2.47, (*) 3.13, (−) 3.85 in units of 10^{13} molecules cm^{-3}.

First, ln A_{Cu} was followed as a function of the reaction time t at various amounts of the reactant added, e.g. CH_3Br, and a linear regression of ln A versus t was carried out. Next, the slopes of these lines were plotted versus $[CH_3Br]$. A weighted linear regression results in a straight line with an intercept of $7.34D_{Cu,Ar}/2r^2$ and a slope equal to k_1/η.

This procedure has been followed for many other reactions studied at our laboratory. It takes into account the uncertainties of several variables such as temperature, flow, reactor radius, and total pressure. By combining these uncertainties according to the method explained by Howard,[19] the uncertainties σ_S and σ_k for the calculated values of the slope S and the rate constant k were calculated. Finally, the systematic error of 10% for the correction factor 1.3 has been added, resulting in the total standard deviation σ_k. The overall precision on the reported values of the rate constants is in the range 15−25%.

The procedure is illustrated in Figure 1, where the natural logarithm of the copper absorbance ln A_{Cu} is plotted against the reaction time for various amounts of CH_3Br added. The experimental conditions were $T_g = 516$ K, the reactor pressure $P_r = 9$ Torr, and the MIP afterglow parameters T_s and $[H_2]$ were set respectively at 537 K and 9.9 mTorr. When the absolute values S of the slopes of these lines are plotted versus the CH_3Br concentration, a straight line is obtained, as is shown in Figure 2. A weighted linear regression yields a value for $k_1 = (2.5 \pm 0.3) \times 10^{-12}$ cm^3 $molecule^{-1}$ s^{-1} and an intercept I of (23.1 ± 0.9) s^{-1} at $T_g = 516$ K.

The points shown at the ordinate in Figure 2 are the observed copper decays in the absence of the coreagent CH_3Br. The pseudo-first-order plots for the experiments at two other temperatures are also shown. The values for k_1 are $(1.2 \pm 0.2) \times 10^{-12}$ and $(5.4 \pm 0.8) \times 10^{-12}$ cm^3 $molecule^{-1}$ s^{-1} at 390 and 702 K, respectively. These results clearly indicate that the rate constant k_1 increases with T_g and will have an activation energy.

Influence of the MIP Afterglow Parameters. The possible influence of a number of MIP afterglow parameters on the magnitude of the derived rate constants has been verified. Experimental conditions and results are summarized in Table 1. Changing the hydrogen content in the MIP afterglow makes it possible to check the influence of excess H atoms on the

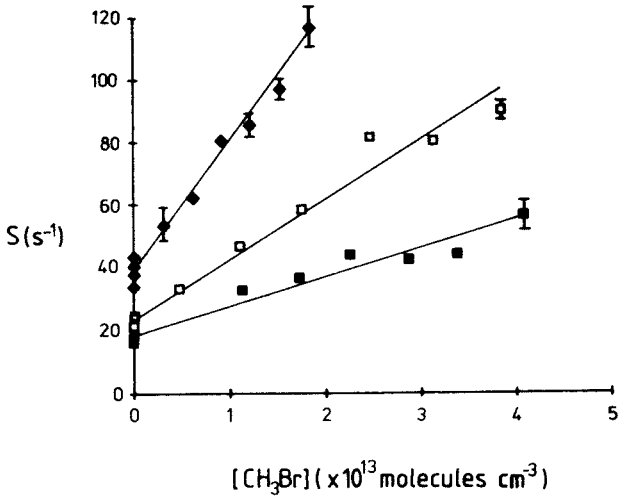

Figure 2. Absolute value S of the slope of eq 5 as a function of CH_3Br concentration for three different temperatures: (■) 390 K, (□) 516 K, (◆) 702 K.

TABLE 1: Influence of the MIP Afterglow Parameters on the Value of k_1 for the Cu + CH_3Br Reaction[a]

T_g (K)	T_s (K)	[H_2] (mTorr)	P_r (Torr)	k_1 (cm^3 molecule^{-1} s^{-1})
		Hydrogen Content [H_2]		
302	513	3.3	9	$(7.7 \pm 1.3) \times 10^{-13}$
300	514	3.3	9	$(7.7 \pm 1.1) \times 10^{-13}$
302	513	32.5	9	$(7.7 \pm 1.1) \times 10^{-13}$
300	514	32.7	9	$(7.7 \pm 1.0) \times 10^{-13}$
512	537	4.9	9	$(2.6 \pm 0.4) \times 10^{-12}$
516	537	9.9	9	$(2.5 \pm 0.3) \times 10^{-12}$
517	538	48.8	9	$(2.6 \pm 0.4) \times 10^{-12}$
519	537	145.8	9	$(2.3 \pm 0.4) \times 10^{-12}$
803	554	8.3	9	$(8.2 \pm 1.1) \times 10^{-12}$
804	553	32.9	9	$(9.1 \pm 1.5) \times 10^{-12}$
		Temperature T_s of the Solid		
302	513	3.3	9	$(7.7 \pm 1.3) \times 10^{-13}$
302	513	3.3	9	$(7.4 \pm 1.0) \times 10^{-13}$
300	525	3.3	9	$(9.5 \pm 1.7) \times 10^{-13}$
304	532	3.3	9	$(8.6 \pm 1.4) \times 10^{-13}$
505	514	4.9	9	$(2.2 \pm 0.3) \times 10^{-12}$
512	537	4.9	9	$(2.6 \pm 0.4) \times 10^{-12}$
512	556	4.9	9	$(2.5 \pm 0.4) \times 10^{-12}$
		Reactor Pressure P_r		
301	513	3.3	7	$(6.7 \pm 1.1) \times 10^{-13}$
304	513	3.3	8	$(7.8 \pm 1.3) \times 10^{-13}$
302	513	3.3	9	$(7.7 \pm 1.3) \times 10^{-13}$
301	513	3.3	10	$(9.0 \pm 1.3) \times 10^{-13}$
301	513	3.3	10	$(7.2 \pm 1.1) \times 10^{-13}$
301	513	3.3	11	$(7.7 \pm 1.1) \times 10^{-13}$
417	514	4.9	7	$(1.4 \pm 0.3) \times 10^{-12}$
404	514	4.7	9	$(1.2 \pm 0.2) \times 10^{-12}$
408	514	4.7	9	$(1.3 \pm 0.2) \times 10^{-12}$
407	514	4.9	11	$(1.1 \pm 0.1) \times 10^{-12}$

[a] T_g, reaction temperature in gas phase; T_s, temperature of the CuCl solid; [H_2], hydrogen content of the MIP; P_r, reaction pressure; microwave power $P_W = 40$ W.

measured rate constant. These H atoms, which are left after the production of Cu atoms, might react with a fraction of the added CH_3Br or with CuBr to regenerate Cu atoms. The results in Table 1 show that there is no systematic effect of the hydrogen content on the derived value of k_1 at temperatures around 300, 516, and 803 K. Therefore, the interference of H atom reactions seems to be negligible under these experimental conditions.

The microwave power was kept constant at 40 W. A variation of this parameter is equivalent to changing the H atom concentration in the MIP afterglow, which as said above had no effect.

TABLE 2: k_1 of the Cu + CH_3Br Reaction as a Function of Temperature[a]

T_g (K)	T_s (K)	[H_2] (mTorr)	P_r (Torr)	k_1 (cm^3 molecule^{-1} s^{-1})
300	514	3.3	9	$(7.7 \pm 1.1) \times 10^{-13}$
300	514	32.7	9	$(7.7 \pm 1.0) \times 10^{-13}$
300	525	3.3	9	$(9.5 \pm 1.7) \times 10^{-13}$
301	513	3.3	7	$(6.7 \pm 1.1) \times 10^{-13}$
301	513	3.3	10	$(7.2 \pm 1.1) \times 10^{-13}$
301	513	3.3	10	$(6.9 \pm 1.0) \times 10^{-13}$
301	513	3.3	10	$(9.0 \pm 1.3) \times 10^{-13}$
301	513	3.3	11	$(7.7 \pm 1.1) \times 10^{-13}$
302	513	3.3	9	$(7.7 \pm 1.3) \times 10^{-13}$
302	513	32.5	9	$(7.7 \pm 1.1) \times 10^{-13}$
302	513	3.3	9	$(6.3 \pm 1.1) \times 10^{-13}$
302	513	3.3	9	$(7.4 \pm 1.0) \times 10^{-13}$
302	514	3.3	9	$(6.6 \pm 1.0) \times 10^{-13}$
304	513	3.3	8	$(7.8 \pm 1.3) \times 10^{-13}$
304	532	3.3	9	$(8.6 \pm 1.4) \times 10^{-13}$
327	522	4.9	9	$(7.0 \pm 1.1) \times 10^{-13}$
344	512	4.7	9	$(8.2 \pm 1.2) \times 10^{-13}$
359	512	4.7	9	$(9.5 \pm 1.5) \times 10^{-13}$
390	522	8.1	9	$(1.2 \pm 0.2) \times 10^{-12}$
404	514	4.7	9	$(1.2 \pm 0.2) \times 10^{-12}$
407	514	4.9	1	$(1.1 \pm 0.1) \times 10^{-12}$
408	514	4.7	9	$(1.3 \pm 0.2) \times 10^{-12}$
417	514	4.9	7	$(1.4 \pm 0.3) \times 10^{-12}$
434	520	5.2	9	$(1.6 \pm 0.2) \times 10^{-12}$
474	520	6.5	9	$(2.1 \pm 0.3) \times 10^{-12}$
505	514	4.9	9	$(2.2 \pm 0.3) \times 10^{-12}$
512	537	4.9	9	$(2.6 \pm 0.4) \times 10^{-12}$
512	556	4.9	9	$(2.5 \pm 0.4) \times 10^{-12}$
516	537	9.9	9	$(2.5 \pm 0.3) \times 10^{-12}$
517	538	48.8	9	$(2.6 \pm 0.4) \times 10^{-12}$
519	537	145.8	9	$(2.3 \pm 0.4) \times 10^{-12}$
562	530	13.0	9	$(2.9 \pm 0.5) \times 10^{-12}$
619	529	13.0	9	$(3.3 \pm 0.6) \times 10^{-12}$
654	514	8.3	8	$(4.5 \pm 2.0) \times 10^{-12}$
702	536	8.1	9	$(5.4 \pm 0.8) \times 10^{-12}$
728	555	13.0	9	$(6.7 \pm 1.3) \times 10^{-12}$
766	549	8.1	9	$(6.6 \pm 1.3) \times 10^{-12}$
798	554	8.3	9	$(7.1 \pm 1.2) \times 10^{-12}$
803	554	8.3	9	$(8.2 \pm 1.1) \times 10^{-12}$
804	553	32.9	9	$(9.1 \pm 1.5) \times 10^{-12}$

[a] Symbols are the same as in Table 1.

As the sublimation of CuCl occurs through the formation of Cu_xCl_x oligomers,[20] a change of the sublimation temperature T_s from 513 to 532 K raises the gas-phase concentration of the Cu_xCl_x oligomers by a factor of 3.2 at $T_g = 302$ K.[9] Around a gas temperature of 510 K the oligomer concentration increases by a factor of 11.7 in the T_s range 514−556 K. The results in Table 1 show that a variation of the temperature T_s of the CuCl pellet does not have any systematic effect on the value of k_1.

Another MIP afterglow parameter is the reactor pressure P_r, which was varied between 7 and 11 Torr. The results in Table 1 indicate that P_r has no systematic effect on the value of k_1. This confirms a second-order character for reaction 2. Moreover, a lower reactor pressure enhances the diffusion of the reagents toward the reactor wall, so the absence of a pressure effect on k_1 leads to the conclusion that hydrodynamic flow characteristics do not have any influence on the value of k_1.

Temperature Dependence of k_1. A summary of the experimental conditions and derived values for k_1 is given in Table 2 in the temperature range from 300 to 804 K. A weighted nonlinear regression on these data yields the Arrhenius expression

$$k_1 = (1.7 \pm 0.2) \times 10^{-11} \exp\left(\frac{-8.2 \pm 0.5 \text{ kJ mol}^{-1}}{RT}\right) \text{cm}^3 \text{ molecule}^{-1} \text{ s}^{-1} \quad (6)$$

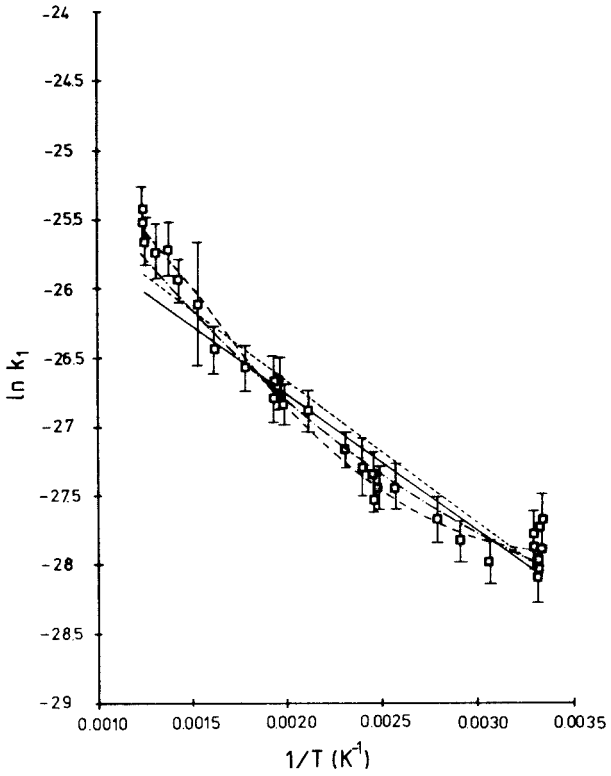

Figure 3. Arrhenius plot of ln k_1 versus $1/T$: Full line (—), nonlinear regression of k_1 versus $1/T$ described by eq 6; dotted line (···), linear regression of ln k_1 versus $1/T$ described by eq 7; dash−dot line (−·−·), nonlinear regression of k_1 versus T according to the three-parameter expression 8 with the value of n fixed at 2 (see Table 3); dashed line (− − −), polynomial expression described by eq 10.

A weighted linear regression of ln k_1 versus $1/T$ results in the expression

$$k_1 = 2.0^{+0.3}_{-0.2} \times 10^{-11} \exp\left(\frac{-8.5 \pm 0.4 \text{ kJ mol}^{-1}}{RT}\right) \text{cm}^3 \text{ molecule}^{-1} \text{ s}^{-1} \quad (7)$$

In Figure 3 the experimentally measured rate constants together with eqs 6 and 7 are plotted as a conventional Arrhenius graph. Both expressions yield consistent Arrhenius parameters, but in view of the symmetric error on the preexponential factor for the nonlinear regression method, expression 6 will be used further in the discussion. However, a slight deviation from linearity can be observed, which indicates non-Arrhenius behavior for reaction 2, as will be discussed in the next section.

Non-Arrhenius Behavior of the Cu + CH_3Br Reaction. The Arrhenius plot of the experimental points in Figure 3 apparently shows a slight curvature, which was also found for the reaction between Cu and CH_3Cl.[8] To describe this non-Arrhenius behavior, three-parameter expressions of the type

$$k(T) = AT^n \exp\left(\frac{-E}{RT}\right) \text{cm}^3 \text{ molecule}^{-1} \text{ s}^{-1} \quad (8)$$

are frequently used.

A weighted nonlinear regression for the values of k_1 in Table 2 leads to the modified Arrhenius equation

$$k_1 = (5 \pm 105) \times 10^{-18} T^{(2.2 \pm 1.0)} \times \exp\left(\frac{-2.4 \pm 0.6 \text{ kJ mol}^{-1}}{RT}\right) \text{cm}^3 \text{ molecule}^{-1} \text{ s}^{-1} \quad (9)$$

TABLE 3: Two-Parameter Fit of the Expression $k(T) = AT^n \exp(-E/RT)$[a]

n (fixed)	A ($\times 10^{-14}$ cm^3 molecule^{-1} s^{-1})	E (kJ mol^{-1})	residual sum of squares
0.5	49.8 ± 6.4	6.5 ± 0.4	60
1	1.5 ± 0.2	4.7 ± 0.4	50
1.5	0.042 ± 0.004	3.0 ± 0.3	41
2	0.0012 ± 0.0001	1.2 ± 0.3	34
2.5	0.000035 ± 0.000003	−0.56 ± 0.25	28

[a] The value of n is fixed for the calculation of A and E. The sum of the squares of the residuals is also given.

The very large standard deviation for the parameter A indicates that a three-parameter fitting procedure is rather unrealistic. Heberger et al.[21] stated that three-parameter expressions derived in this way are to be considered as merely a representation of experimental points, which should be used only for interpolation or extrapolation of the rate coefficient values.

In another approach one parameter can be fixed, which reduces the fitting to a two-parameter problem. In analogy with the reaction between Cu and CH_3Cl,[8] n is fixed in the range between 0.5 and 2.5, and values for the two remaining parameters A and E are calculated with increments for n of 0.5. The results, summarized in Table 3, show that the sum of squares of the residuals decreases with an increasing value for n. Moreover, the standard deviations on the parameter A are much smaller than in the three-parameter fit of eq 9. It should be noticed that the preexponential factor $A = (5 \pm 105) \times 10^{-18}$ cm^3 molecule^{-1} s^{-1} and the activation energy $E = 2.4 \pm 0.6$ kJ mol^{-1} given in eq 9 fall within the range of values mentioned in Table 3 when the error of ±1.0 for $n = 2.2$ in eq 9 is taken into account. As an example, an Arrhenius plot using the parameter set for $n = 2$ is shown in Figure 3. The figure illustrates that the three-parameter expression considerably improves the fit of the experimental points.

As was shown for the Cu + CH_3Cl reaction,[8] rigorous transition state theory calculations allowed us to refine the exact value of n. Ab initio molecular orbital calculations at the Hartree−Fock level were used to obtain vibrational frequencies and moments of inertia of CH_3Cl and the transition state Cu−Cl−CH_3. Analogous calculations of the transition state Cu−Br−CH_3 have not yet been carried out at that level. In view of the uncertainty on the value of n between 0.5 and 2.5 an energy barrier for reaction 2 in the range 3 ± 3.5 kJ mol^{-1} may be adopted.

The experimentally measured values of k_1 can even be fit better as a function of temperature by means of the polynomial expression 10, as is also illustrated in Figure 3:

$$\log k_1(T) = +223.6669 - 264.2058(\log T) + 97.7693(\log T)^2 - 11.9244(\log T)^3 \quad (10)$$

Non-Arrhenius behavior is also observed when different reaction channels, leading to the formation of reaction products in various electronic states, are accessible. In reaction 2, however, CuBr is formed in its electronic ground state X $^1\Sigma^+$ because the reaction exothermicity of 37.6 kJ mol^{-1} does not allow the formation of the lowest electronically excited state lying at 245 kJ mol^{-1} above the ground state.[22]

Cu + CH_3I Reaction. The same experimental procedure as described for the Cu + CH_3Br reaction was followed to study the reaction between Cu and CH_3I.

TABLE 4: Influence of the MIP Afterglow Parameters on the Value of k_2 for the Cu + CH_3I Reaction[a]

T_g (K)	T_s (K)	[H_2] (mTorr)	P_r (Torr)	k_2 (cm^3 molecule^{-1} s^{-1})
		Hydrogen Content [H_2]		
300	537	5.0	9	$(5.7\pm0.8) \times 10^{-11}$
300	537	12.9	9	$(6.2\pm0.8) \times 10^{-11}$
300	536	50.4	9	$(6.0\pm0.8) \times 10^{-11}$
522	525	5.0	9	$(7.5\pm1.1) \times 10^{-11}$
522	525	15.2	9	$(7.3\pm1.1) \times 10^{-11}$
524	525	30.0	9	$(6.4\pm1.0) \times 10^{-11}$
522	525	50.4	9	$(6.4\pm1.0) \times 10^{-11}$
		Temperature T_s of the Solid		
300	508	5.0	9	$(5.2\pm0.7) \times 10^{-11}$
300	514	5.0	9	$(5.9\pm0.8) \times 10^{-11}$
300	526	5.0	9	$(5.8\pm0.8) \times 10^{-11}$
300	531	5.0	9	$(5.8\pm0.8) \times 10^{-11}$
300	537	5.0	9	$(5.7\pm0.8) \times 10^{-11}$
527	511	5.0	9	$(6.9\pm1.3) \times 10^{-11}$
524	518	5.0	9	$(6.4\pm1.3) \times 10^{-11}$
522	525	5.0	9	$(7.5\pm1.1) \times 10^{-11}$
516	538	5.0	9	$(6.0\pm1.1) \times 10^{-11}$
		Reactor Pressure P_r		
300	534	12.9	7	$(5.8 \pm 1.0) \times 10^{-11}$
300	535	12.9	8	$(5.8 \pm 0.8) \times 10^{-11}$
300	537	12.9	9	$(6.2 \pm 0.8) \times 10^{-11}$
300	537	12.9	11	$(5.4 \pm 0.8) \times 10^{-11}$
418	516	5.0	7	$(7.6 \pm 1.2) \times 10^{-11}$
415	516	5.0	8	$(6.0 \pm 0.8) \times 10^{-11}$
417	516	5.0	9	$(6.8 \pm 0.9) \times 10^{-11}$
412	516	5.0	10	$(6.3 \pm 0.8) \times 10^{-11}$
406	516	5.0	11	$(6.3 \pm 0.8) \times 10^{-11}$

[a] Symbols are the same as in Table 1.

First, the possible influence of a number of MIP afterglow parameters on the derived value of k_2 was checked. Experimental conditions and results are given in Table 4. The results indicate again that neither the concentration of molecular hydrogen, nor the temperature T_s of the solid, nor the reactor pressure P_r have any systematic effect on the value of k_2.

Next, the rate constant k_2 was measured between 300 and 696 K. Table 5 summarizes the experimental conditions and derived values for k_2.

A weighted nonlinear regression gives the Arrhenius expression

$$k_2 = (7.9 \pm 0.5) \times 10^{-11} \exp\left(\frac{-0.8 \pm 0.2 \text{ kJ mol}^{-1}}{RT}\right) \text{cm}^3 \text{ molecule}^{-1} \text{ s}^{-1} \quad (11)$$

Because of the symmetric error, eq 11 is preferred to a linear regression. The expression and the experimentally derived rate constants are illustrated on an Arrhenius plot in Figure 4. The error ranges for the experimental points may seem large, but this is only due to the scale chosen for ln k_2. As a matter of fact, the standard deviations for k_2 in Table 5 vary between 13 and 23%, which is comparable to the values for the Cu + CH_3-Br reaction. Although a slight deviation from linearity was observed for the Cu + CH_3Cl and CH_3Br reactions, non-Arrhenius behavior does not seem to occur in the case of the reaction between Cu and CH_3I.

In addition the value of k_2 is high taking into account that the enthalpy of reaction 3 $\Delta H_r = +38.6 \pm 21.5$ kJ mol^{-1}. The reaction enthalpy ΔH_r is calculated using values given in the JANAF tables[23] and dissociation energies in ref 24. This large uncertainty is mainly due to the value of the dissociation energy of CuI, which is quoted as 197 ± 21 kJ mol^{-1}.[24] But even when the highest value of 218 kJ mol^{-1} is taken for the dissociation energy of CuI, the reaction Cu + CH_3I stays endothermic by 17.6 kJ mol^{-1}, and one would have an activation energy of at least the same magnitude. The activation energy of 0.8 ± 0.2 kJ mol^{-1} derived in our work cannot be reconciled with the available thermochemical data for the reaction between Cu and CH_3I. However, the situation could become quite different if the value of 3 eV is taken for the CuI dissociation energy.[25] In this case reaction 3 becomes exothermic for -53.4 kJ mol^{-1}, and a small activation energy for the reaction is entirely plausible.

TABLE 5: k_2 of the Cu + CH_3I Reaction as a Function of Temperature[a]

T_g (K)	T_s (K)	[H_2] (mTorr)	P_r (Torr)	k_2 (cm^3 molecule^{-1} s^{-1})
300	508	5.0	9	$(5.2 \pm 0.7) \times 10^{-11}$
300	514	5.0	9	$(5.9 \pm 0.8) \times 10^{-11}$
300	515	4.7	9	$(5.1 \pm 0.7) \times 10^{-11}$
300	526	5.0	9	$(5.8 \pm 0.8) \times 10^{-11}$
300	531	5.0	9	$(5.8 \pm 0.8) \times 10^{-11}$
300	534	12.9	7	$(5.8 \pm 1.0) \times 10^{-11}$
300	535	12.9	8	$(5.8 \pm 0.8) \times 10^{-11}$
300	536	50.4	9	$(6.0 \pm 0.8) \times 10^{-11}$
300	537	5.0	9	$(5.7 \pm 0.8) \times 10^{-11}$
300	537	12.9	9	$(6.2 \pm 0.8) \times 10^{-11}$
300	537	12.9	11	$(5.4 \pm 0.8) \times 10^{-11}$
339	513	5.0	9	$(5.6 \pm 0.8) \times 10^{-11}$
360	527	5.0	9	$(5.6 \pm 1.0) \times 10^{-11}$
393	527	5.0	9	$(5.3 \pm 0.9) \times 10^{-11}$
406	516	5.0	11	$(6.3 \pm 0.8) \times 10^{-11}$
412	516	5.0	10	$(6.3 \pm 0.8) \times 10^{-11}$
415	516	5.0	8	$(6.0 \pm 0.8) \times 10^{-11}$
417	516	5.0	9	$(6.8 \pm 0.9) \times 10^{-11}$
418	516	5.0	7	$(7.6 \pm 1.2) \times 10^{-11}$
433	513	5.0	9	$(5.6 \pm 0.9) \times 10^{-11}$
472	527	5.0	9	$(5.6 \pm 0.9) \times 10^{-11}$
516	538	5.0	9	$(6.0 \pm 1.1) \times 10^{-11}$
522	525	5.0	9	$(7.5 \pm 1.1) \times 10^{-11}$
522	525	15.2	9	$(7.3 \pm 1.1) \times 10^{-11}$
522	525	50.4	9	$(6.4 \pm 1.0) \times 10^{-11}$
524	518	5.0	9	$(6.4 \pm 1.3) \times 10^{-11}$
524	525	30.0	9	$(6.4 \pm 1.0) \times 10^{-11}$
527	511	5.0	9	$(6.9 \pm 1.3) \times 10^{-11}$
550	513	5.0	9	$(5.5 \pm 1.1) \times 10^{-11}$
562	538	5.0	9	$(5.3 \pm 1.1) \times 10^{-11}$
599	527	10	9	$(6.9 \pm 1.6) \times 10^{-11}$
605	527	5.0	9	$(8.2 \pm 1.2) \times 10^{-11}$
661	514	5.0	9	$(7.4 \pm 1.0) \times 10^{-11}$
696	526	5.0	10	$(6.2 \pm 1.3) \times 10^{-11}$

[a] Symbols are the same as in Table 1.

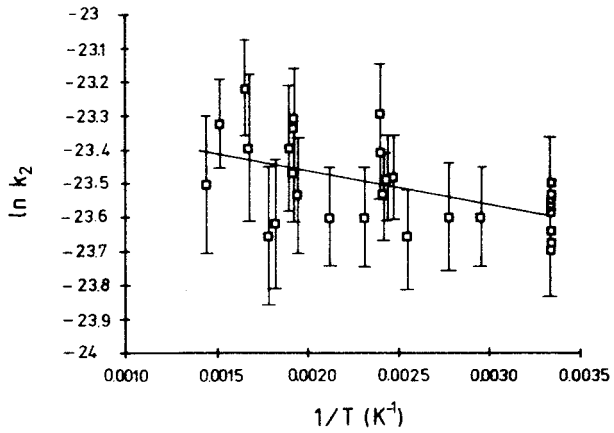

Figure 4. Arrhenius plot of ln k_2 versus $1/T$: Full line (—), nonlinear regression of k_2 versus $1/T$ described by eq 11.

Discussion

Since the kinetics of the reaction between Cu atoms and CH_3-Cl has already been investigated,[8] this publication adds the

TABLE 6: Arrhenius Parameters *A* and *E* for the Reactions Me + RX → MeX + R with the Temperature Range, the Vertical Electron Affinity EA_v of RX,[29,31,32] and the Dissociation Energy *D*(C−X) for the C−X Bond in RX.[24] The Values of *E* with (*) Are Obtained Using the Three-Parameter Expression 8

			Cu + CH_3X			K + CH_3X			
RX	EA_v (eV)	*D*(C−X) (kJ mol^{-1})	*T* (K)	*A* (cm^3 $molecule^{-1}$ s^{-1})	*E* (kJ mol^{-1})	*T* (K)	*A* (cm^3 $molecule^{-1}$ s^{-1})	*E* (kJ mol^{-1})	ref
CH_3F	−6.2	452				822−922	$1.9^{+1.1}_{-0.7} \times 10^{-10}$	59 ± 3.3	27
CH_3Cl	−3.45	351	389−853	$(1.7 \pm 0.4) \times 10^{-11}$	34.4 ± 1.1 24.8*	831−917	$3.2^{+2.0}_{-1.2} \times 10^{-10}$	32 ± 3.6	28
CH_3Br	−0.5	293	300−804	$(1.7 \pm 0.2) \times 10^{-11}$	8.2 ± 0.5 3 ± 3.5*	798−903	$1.7^{+0.3}_{-0.2} \times 10^{-10}$	15.9 ± 1.2	27
CH_3I	0.3	236	300−696	$(7.9 \pm 0.5) \times 10^{-11}$	0.8 ± 0.2			0	33

TABLE 7: Calculated r_c Values for the Reactions Cu + RX → CuX + R. The Values Are Obtained Using the Expression $A = Q_r v_r = \pi(r_c)^2 v_r$, the Vertical Electron Affinity EA_v of RX,[29,31] and the Adiabatic Electron Affinity EA_{ad} of RX[26]

Cu + RX	*A* (cm^3 $molecule^{-1}$ s^{-1})	v_r (m s^{-1})	Q_r (Å^2)	r_c (Å)	EA_v(RX) (eV)	r_c (Å)	EA_{ad}(RX) (eV)	r_c (Å)
Cu + CH_3Cl	$(1.7 \pm 0.4) \times 10^{-11}$	475	3.58	1.07	−3.45	1.29	0.1	1.89
Cu + CH_3Br	$(1.7 \pm 0.2) \times 10^{-11}$	408	4.16	1.15	−0.5	1.75	0.4	1.97
Cu + CH_3I	$(7.9 \pm 0.5) \times 10^{-11}$	380	20.77	2.57	0.3	1.94	0.6	2.02

results for the reaction of Cu with CH_3Br and CH_3I. Consequently, it is possible to check the effect of electronegative substituents on the reactivity of methyl halides for a number of metal atom reactions. The Arrhenius parameters, i.e. the preexponential factor *A* and the activation energy *E*, are given in Table 6.

Regarding the three copper atom reactions studied, no other kinetic data are presently available in the literature for comparison. In contrast, reactions of alkyl halides RX with alkali-metal atoms have been investigated in more detail for more than 60 years. The electron-jump model was introduced to explain the reactivity of Na atoms with halomethanes.[4,5] The reaction between the metal Me and CH_3X is initiated by a sudden electron jump from Me to CH_3X in the vicinity of the crossing between the covalent and ionic potentials. As an approximation, it is reasonable to assume that the CH_3X molecule is unaware of the presence of the Me atom just before the electron jump and that the CH_3X^- molecular ion represents the initial state of the product immediately after the electron jump. Under such conditions, the multidimensional potential surfaces can be replaced by a potential-energy curve as a function of the C−X bond distance for both the CH_3X molecule and the CH_3X^- molecular ion. K. T. Wu[26] has estimated potential-energy barriers for the reactions of alkali atoms with various methyl halides, based on this model.

The discussion will be limited to the reactions of Cu and K with the methyl halides since both atoms have an electronic configuration with one 4s electron in the outer shell. Arrhenius expressions for *K*[27,28] have only been derived in rather limited temperature ranges from 798 to 922 K, and the parameters are also shown in Table 6. Previous studies of metal atom reactions with Cl_2[13,16] have indicated that the electron-jump mechanism is characterized by a large preexponential factor *A* and a low activation energy *E*. Since the reaction of Cu with CH_3Cl has a preexponential factor of only (1.7 ± 0.4) × 10^{-11} cm^3 $molecule^{-1}$ s^{-1} and the activation energy *E* is 34.4 ± 1.1 kJ mol^{-1}, the electron-jump mechanism could be ruled out.[8] This is confirmed by considering the distance r_c at which the electron transfer should occur. A value for r_c can be calculated in two ways. On the one hand, the experimentally derived preexponential factor *A* can be used to calculate reaction cross sections Q_r and thus also r_c values using the expression $A = Q_r v_r = \pi(r_c)^2 v_r$. The values obtained are given in Table 7.

On the other hand, r_c can be calculated using expression 1. It has been mentioned[16] that for large values of r_c the vertical electron affinity EA_v has to be used, while for small r_c values the adiabatic electron affinity EA_{ad} is more appropriate. In Table 7 the results for both electron affinities are shown. The values of EA_{ad} are derived from a figure in ref 26 which represents the potential-energy curve as a function of the C−X bond distance for both the CH_3X molecule and the CH_3X^- molecular ion. These curves were calculated using the Morse potential for the molecule and Wentworth's empirical potential-energy function for the negative ion.

The preexponential factor *A* for the reaction between Cu and CH_3Cl corresponds to a distance r_c of 1.07 Å. Inserting IE(Cu) = 7.7 eV[24] and $EA_v(CH_3Cl) = -3.45$ eV[29] in eq 1, one arrives at an r_c value of 1.29 Å, while with $EA_{ad}(CH_3Cl) = 0.1$ eV[26] r_c becomes equal to 1.89 Å. Since the experimentally derived r_c is smaller than the theoretically calculated values and all these r_c values are smaller than the equilibrium distance r_e in the molecule CuCl (r_e(Cu−Cl) = 2.05 Å),[23] it is obvious that the reaction Cu + CH_3Cl does not occur according to the electron-jump mechanism.

For a metal atom reaction with CH_3Br the activation energy *E* is smaller compared to the CH_3Cl reactions, as can be seen in Table 6. However, the preexponential factor for Cu + CH_3Br is as small as for Cu + CH_3Cl, which results again in an r_c smaller than the values calculated using EA_v and EA_{ad}. Therefore, the electron-jump mechanism can be excluded here too.

As is shown in Table 6, the reaction between Cu + CH_3I has a low activation energy *E* of 0.8 ± 0.2 kJ mol^{-1}. The preexponential factor *A* is (7.9 ± 0.5) × 10^{-11} cm^3 $molecule^{-1}$ s^{-1}, which results in an r_c of 2.57 Å. In this case, the experimentally derived r_c is larger than 1.94 Å and 2.02 Å, calculated with EA_v and EA_{ad} respectively. These data might indicate an electron-jump mechanism. However, it is clear that the *A* factor is lower than for other metal atom−halogen reactions. For instance, the reaction between Cu and Cl_2[13] has a preexponential factor $A = 3.3 \times 10^{-10}$ cm^3 $molecule^{-1}$ s^{-1}. This can simply be explained by the values of the vertical electron affinity of 0.3 eV for CH_3I compared to the much larger value of 1 eV for Cl_2. Considering this and the fact that the r_c values are smaller than 3 Å, a close-range electron-transfer mechanism is proposed for the Cu + CH_3I reaction.

For the reaction between K and CH_3Cl the activation energy is comparable to the value for Cu, but the preexponential factor is a factor of 10 higher. With the vertical electron affinity of CH_3Cl (−3.45 eV)[26] and the ionization energy for K (4.3 eV)[24]

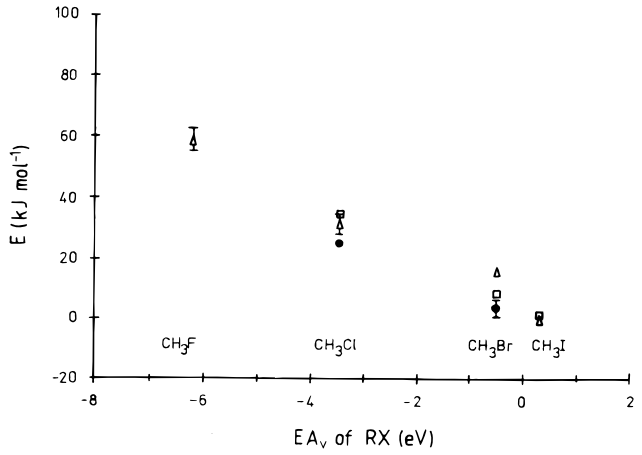

Figure 5. Activation energy E for the reactions Me + RX → MeX + R (given in Table 6) as a function of the vertical electron affinity EA_v of RX (□ Cu; △ K; ● Cu with E obtained using the three-parameter expression).

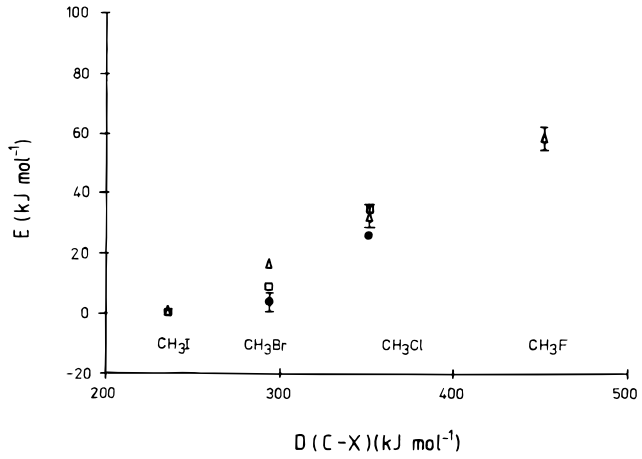

Figure 6. Activation energy E for the reactions Me + RX → MeX + R (given in Table 6) as a function of the dissociation energy of the C−X bond in RX (□ Cu; △ K; ● Cu with E obtained using the three-parameter expression).

an r_c value of 1.85 Å is obtained. In case the adiabatic electron affinity of CH_3Cl (=0.1 eV)[26] is used, r_c is 3.42 Å. The results indicate that the electron jump might take place over a rather short distance. For the reactions of K with CH_3Br and CH_3I, the electron jump occurs over longer distances.

K. T. Wu[26] has estimated potential-energy barriers for the reactions of alkali atoms with various methyl halides, on the basis of the electron-jump model. The values obtained are 183, 52, 24, and 2.5 kJ mol^{-1} for Me + CH_3F, CH_3Cl, CH_3Br, and CH_3I, respectively, so the barrier decreases as the halogen changes from F to I. A comparison of these theoretically calculated values with the experimentally measured activation energies in Table 6 reveals a remarkable difference. However, the experimentally determined values do decrease from CH_3F to CH_3I.

For several types of reactions correlations have been observed between the reactivity and the ability of reagents to accept electrons described by their electron affinity EA.[30] Table 6 shows a strong negative correlation between the activation energy E of the reaction and the vertical electron affinity EA_v of RX, as is also illustrated in Figure 5. The activation energy E of the Me + RX reactions can also be related to the dissociation energy D(C−X) of the C−X bond in the molecule RX. As can be seen in Table 6 and as is illustrated in Figure 6, a good correlation is observed between the magnitude of the activation energy of the reactions and the bond strength of the methyl halides.

It may be reasonable to conclude that the harpooning mechanism, which successfully describes alkali metal−methyl halide reactions, cannot provide a quantitative approach for the copper atom reactions with methyl chloride and bromide. For these reactions the electron-jump mechanism can be excluded. On the other hand, it can be stated that the reaction between Cu and CH_3I occurs according to a close-range electron-transfer mechanism. The good correlation between the activation energy and the dissociation energy of the C−X bond in RX is rather an indication for an atom-transfer mechanism.

Acknowledgment. The authors are grateful to the Joint Fund for Basic Research (FKFO) for a research grant. I.V. was a Research Assistant of the Fund for Scientific Research (FWO), Flanders. C.V. is a Research Director of the FWO.

References and Notes

(1) Polanyi, M.; *Atomic Reactions*; Williams and Norgate Ltd.: London, 1932.
(2) Parrish, D. D.; Herm, R. R. *J. Chem. Phys*. **1971**, *54*, 2518.
(3) Weiss, P. S.; Mestdagh, J. M.; Schmidt, H.; Covinsky, M. H.; Lee, Y. T. *J. Phys. Chem*. **1991**, *95*, 3005.
(4) Herschbach, D. R. *Adv. Chem. Phys*. **1966**, *10*, 319.
(5) Ogg, R. A.; Polanyi, M. *Trans. Faraday Soc*. **1935**, *31*, 1375.
(6) Warhurst, E. *Q. Rev. Chem. Soc*. **1951**, *5*, 44.
(7) Haresnape, J. N.; Stevels, J. M.; Warhurst, E. *Trans. Faraday Soc*. **1940**, *36*, 465.
(8) Vinckier, C.; Vanhees, I.; Sengupta D.; Nguyen M. T. *J. Phys. Chem*. **1996**, *100*, 8302.
(9) Vinckier, C.; Dumoulin, A.; Corthouts, J.; De Jaegere, S. *J. Chem. Soc., Faraday Trans. 2* **1988**, *84*, 1725.
(10) Vinckier, C.; Corthouts, J.; De Jaegere, S. *J. Chem. Soc., Faraday Trans. 2*, **1988**, *84*, 1951.
(11) Vinckier, C.; Verhaeghe, T.; Vanhees, I. *J. Chem. Soc. Faraday Trans*.**1994**, *90*, 2003.
(12) SAS statistical package; SAS Institute Inc.: Cary, NC, 1992.
(13) Vinckier, C.; Verhaeghe, T.; Vanhees, I. *J. Chem. Soc., Faraday Trans*. **1996**, *92*, 1455.
(14) Vinckier, C.; Dumoulin, A.; De Jaegere, S. *J. Chem. Soc., Faraday Trans. 2* **1991**, *87*, 1075.
(15) Vinckier, C.; Christiaens, P. *J. Phys. Chem*. **1992**, *96*, 2146.
(16) Vinckier, C.; Christiaens, P. *J. Phys. Chem*. **1992**, *96*, 8423.
(17) Talcott, C. L.; Ager, J. W., III; Howard, C. J. *J. Chem. Phys*. **1986**, *84*, 6161.
(18) Fontijn, A.; Felder, W. In *Reactive Intermediates in the Gas Phase, Generation and Monitoring*; Setser, D.W., Ed.; Academic Press: New York, 1979; Chapter 2.
(19) Howard, C. J. *J. Phys. Chem*. **1979**, *83*, 3.
(20) Guido, M.; Balducci, G.; Gigli, G.; Spoliti, M. *J. Chem. Phys*. **1971**, *55*, 4566.
(21) Heberger, K.; Kemény, S.; Vidóczy, T. *Int. J. Chem. Kinet*. **1987**, *19*, 171.
(22) Herzberg, G. *Molecular Spectra and Molecular Structure I: Spectra of Diatomic Molecules*; Van Nostrand Reinhold Co., Inc.: New York, 1950.
(23) JANAF Thermochemical Tables; *J. Phys. Chem. Ref. Data* **1985**, *14*, Suppl. 1.
(24) Weast, R. C.; Astle M. J. *CRC Handbook of Chemistry and Physics*; CRC Press: Boca Raton, FL, 1996−1997.
(25) Radzig, A. A.; Smirnov, B. M. *Reference Data on Atoms, Molecules and Ions*; Springer: Berlin, 1985.
(26) Wu, K. T. *J. Phys. Chem*. **1979**, *83*, 1043.
(27) Husain, D.; Lee, Y. H. *Int. J. Chem. Kinet*. **1988**, *20*, 223.
(28) Husain, D.; Lee, Y. H. *J. Photochem. Photobiol. A: Chem*. **1988**, *42*, 13.
(29) Burrow, P. D.; Modelli, A.; Chiu, N. S.; Jordan, K. D. *J. Chem. Phys*. **1982**, *77*, 2699.
(30) Abbatt, J. P. D.; Toohey, D. W.; Fenter, F. F.; Stevens, P. S.; Brune, Wm. H.; Anderson, J. G. *J. Phys. Chem*. **1989**, *93*, 1022.
(31) Moutinho, A. M. C.; Aten, J. A.; Los, J. *Chem. Phys*. **1974**, *5*, 84.
(32) Giordan, J. C.; Moore, J. H.; Tossell, J. A. *Accounts Chem. Res*. **1986**, *19*, 281.
(33) Kerr, J. A.; Lissi, E. A.; Trotman-Dickenson, A. F. *J. Chem. Soc*. **1964**, *2*, 1673.